Mixing of multiple hydrogen plasma beams in a strong magnetic field by $E \times B$ drift-induced rotation

Plasma Phys. Control. Fusion **53** (2011) 105013 (12pp) doi:10.1088/0741-3335/53/10/105013

Mixing of multiple hydrogen plasma beams in a strong magnetic field by $E \times B$ drift-induced rotation

E Oyarzabal[1,3], W A J Vijvers[2], R S Al[2], H J van der Meiden[2], M J van der Pol[2], F L Tabarés[1] and G J van Rooij[2]

[1] TechnoFusion Team. As. Euratom-Ciemat. Av. Complutense 22, 28040 Madrid, Spain
[2] FOM Instituut voor Plasmafysica Rijnhuizen, EURATOM Association, Trilateral Euregio Cluster, PO Box 1207, 3430 BE Nieuwegein, The Netherlands

E-mail: eider.oyarzabal@ciemat.es

Received 31 March 2011, in final form 2 August 2011
Published 22 September 2011
Online at stacks.iop.org/PPCF/53/105013

Abstract
Mixing of up to three ∼1 cm diameter plasma beams of pure hydrogen as well as mixtures of hydrogen and argon in magnetic fields of <1.6 T are studied. An external ring electrode is used to create a radial electric field that induces $E \times B$ rotation of the individual beams around a common axis. Rotation profiles with maximum speeds up to 10 km s^{-1} are measured from the hydrogen atomic line shapes and confirm rotation around the ring axis. Mixing to a total beam diameter of ∼2.5–3 cm is observed in density profiles measured with Thomson scattering near a target at 0.5 m downstream. Currents of up to 60 A were received by the ring, involving an addition power input of up to 5.4 kW to the plasma.

(Some figures in this article are in colour only in the electronic version)

1. Introduction

A plasma of hydrogen isotopes, confined at >150 Million K by magnetic fields, will be the heart of fusion reactors such as ITER [1]. These will use a magnetic field topology such that the outer layer of the plasma exhausts to a special area of the plasma chamber, the divertor. Here, the plasma is neutralized and pumped off. The particle and energy fluxes are determined by the transport from the hot plasma core. The numbers that are foreseen for ITER are 10^{24} ions m^{-2} s^{-1} and 10 MW m^{-2} to the strike zones in the divertor, corresponding to plasma densities close to the wall of 10^{21} m^{-3} at temperatures of a few eV [2]. A surface that can handle such fluxes in steady state is a major research challenge for fusion reactors and a priority for ITER.

[3] U.N.E.D. Ciudad Universitaria, S/N, 28040, Madrid.

The linear plasma generator Magnum-PSI (MAGnetized plasma generator and NUMerical modelling for Plasma Surface Interaction studies) is being developed to study 'plasma surface interaction' (PSI) issues under conditions relevant for the ITER divertor [3]. The achievement of high density-low temperature plasmas is of fundamental importance for this device. Experiments on its forerunner Pilot-PSI have demonstrated that it is indeed possible to produce the required plasma conditions with a cascaded arc plasma source in a magnetic field of 1.6 T [4]. This cascaded arc source is based on the flowing arc developed by Sanden *et al* [5]. The high pressure discharge conditions induced by the large gas flows are in contrast with the low pressure sources that are generally applied in linear plasma devices [6–8]. A remaining challenge resides in increasing the diameter of the plasma beam (∼12 mm at the moment), which is needed to perform experiments at ITER relevant system sizes. The present aim is a beam diameter of ∼5 cm FWHM so that molecules and dust particles that come off the surface are confined and remain part of the PSI system.

A similar goal has been addressed for the design of the Plasma Ablation and LOading of MAterials (PALOMA) facility at the TechnoFusion laboratories in Madrid [9], in which the simultaneous effect of hydrogen saturation from the linear plasma device and pulsed, ELM-like, heat loads from a quasi-stationary plasma accelerators (QSPA) on fusion relevant materials will be investigated. Again, a beam diameter of 5 cm has been envisaged for the corresponding linear plasma device in order to match the plasma gun beam interaction area and to account for possible redeposition effects.

Different approaches are being studied to obtain a larger beam diameter than the natural diameter of ∼12 mm [10]. One of these is based on the use of multiple discharge channels [11]. Mixing of the individual plasma beams emanating from a three-channel source proved not to be trivial, especially for hydrogen plasma, due to fast recombination in the plasma beam edges via molecular processes. In this contribution we investigate beam mixing by the application of an external (i.e. well outside the plasma source) ring electrode. The rationale is that biasing of the ring electrode will enforce a radial current and thus a strong radial electric field that induces fast $E \times B$ rotation of the plasma beams about a common axis. Previous results indicated that this concept works for the case of argon plasma [11].

The aim of this work is to characterize the rotation that can be enforced with an external ring electrode on a set of three magnetized hydrogen plasma beams and the degree of mixing that can be obtained in this way. A cascaded arc with a triangular arrangement of three discharge channels is operated on hydrogen, sometimes with argon added for stabilization of the discharge. The mixing is studied for different distances between the source and the ring in a scan of the magnetic field strength and the plasma source operation parameters. The rotation is determined from Doppler shifts of the hydrogen atom lines around 485 nm. The mixing is characterized with Thomson scattering and continuum light imaging.

2. Experimental set-up

The experiments are performed in the linear plasma generator Pilot-PSI, which has been described in detail before [4, 12]. The design of the three-channel cascaded arc source that has been used in the present experiments is the same as used before [11] and is schematically shown in figure 1. A stack of five insulated copper plates, each having three holes of 5 mm in diameter with 20 mm distance between the holes, forms three discharge channels of 36 mm length. Each channel is provided with a cathode that is inserted into the gas chamber in front of the channel through which the discharge gas is supplied. The gas flow is controlled separately for each channel. The anode is made of a composite consisting of 25% copper and 75% tungsten and contains holes of 5 mm in diameter that continue the discharge channel. The plates are

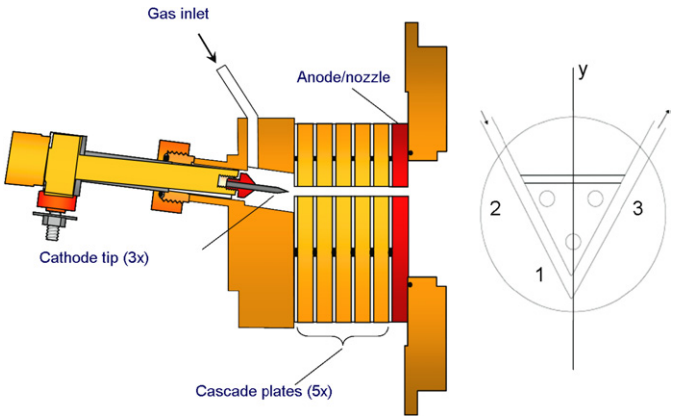

Figure 1. Schematic of the three-channel cascaded arc source. The off centre holes in 5 water cooled electrically insulated cascade plates form three discharge channels, each provided with a cathode and a separately controlled gas flow.

electrically insulated from each other, from the cathode chamber and from the anode plate, by boron-nitride plates of 1 mm thickness. Viton O-rings provide the vacuum sealing of the arc. The 2 mm diameter water cooled cathodes are made of thoriated tungsten and are placed under 7° with respect to the channel axis. The cascade plates are cooled via a triangular cooling channel as sketched in figure 1. The water flow through each plate is typically 8 l min^{-1}. The disadvantage of this non-symmetric water cooling scheme is decreased cooling efficiency in the centre of the plates where power arrives from all discharge channels.

The ring electrode was of 35 mm inner diameter and was positioned either 4 cm or 6 cm downstream from the source nozzle. The ring was made of the same copper–tungsten alloy as the anode plate.

Experiments are performed in a scan of the plasma parameters for different numbers of discharge channels in operation and for two different positions of the ring electrode, i.e. 4 cm and 6 cm away from the source. A linear current ramp of 0.5 s duration to a nominal current of 20 A (held constant for 3 s) for each channel that is in operation is applied to the ring. A voltage limitation of 90 V is used so that the current that can actually be achieved at the maximum voltage depends on the plasma parameters and the distance of the ring from the source.

The plasma is characterized with the following techniques. A Phantom v7.0 CMOS camera (400 × 600 pixels) equipped with optical filters (band pass filters transmitting between 632 nm and 678 nm for Balmer α, between 472 nm and 498 nm for Balmer β, and between 710 and 885 nm for continuum radiation as a qualitative measure of the electron density, respectively) is used for imaging of the plasma beam around the ring electrode. Optical emission spectroscopy (OES) [13] is employed to detect the Doppler shifts and to analyse the line profile of the H_β line. Thomson scattering is used to obtain the density profile of the beam at 2 cm in front of the target, i.e. 0.5 m downstream from the source. A sketch of the line of sights relative to the plasma beams of the Thomson scattering and the high-resolution OES is shown in figure 2.

For OES, a chord of plasma light perpendicular to the plasma axis is collected between the source and the ring electrode at a magnification of 0.4 and imaged onto an array of 40 individual 0.4 mm diameter quartz fibres. The fibre array relays the plasma light to a single-pass $f = 2250$ mm spectrometer in Littrow configuration equipped with a 1024 × 1024 pixels CCD camera. In this way, spatial information is preserved and a spectral range of approximately 1 nm can be investigated over the entire 3–4 cm width of the plasma beam profiles simultaneously.

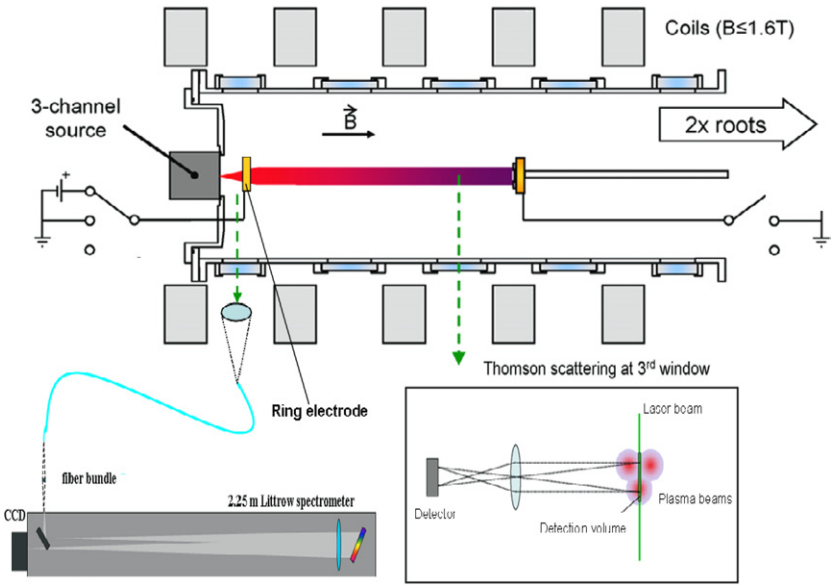

Figure 2. The arrangement of the high-resolution OES and the Thomson scattering diagnostic lines of sight with respect to the plasma in Pilot-PSI. The ring electrode can be connected to a positive voltage, to ground or stay floating.

The exposure time of the CCD camera is typically 1 s and fast temporal fluctuations are thus averaged.

The Thomson scattering diagnostic, which has been discussed in detail elsewhere [14], uses a detection system with a similar fibre array and produces similarly profiles of electron density and temperature over the entire width of the plasma beam.

3. Results

Table 1 gives an overview of the experiments that were carried out in terms of the channels in operation, the gas flow applied per channel, the distance between the source anode and the ring, and the magnetic field strength. For each experiment, the current received by the ring (either due to the imposed current limit of 20 A per operating discharge channel or voltage limited of 90 V) is given. The discharge current is 165 A in each channel that is in operation and thus a total source current of 495 A is achieved with all channels on.

3.1. Dependence of the ring current under the experimental conditions

Table 1 shows that the maximum current that can be achieved at a certain voltage depends mainly on the total discharge current. This observation is in line with the qualitative observation that the total discharge current is a measure of the extent to which the ring is filled with plasma [11]. The ring current decreases at the highest magnetic fields. Earlier work showed that the plasma beam diameter of a single channel decreases with magnetic field strength [4]. We therefore interpret the decreasing ring current with magnetic field as a consequence of the reduction in diameter of the individual plasma beams, i.e. also as a consequence of the lower filling of the ring with plasma. The increase in the current with the ring distance confirms the

Table 1. Overview of the experimental settings that were investigated: the channels in operation, the gas flow applied per channel, the distance between the source anode and the ring and the magnetic field strength. For each experiment, the current that was received by the ring given the 90 V voltage limitation is given.

Channels operated	Gas flow	Ring distance (cm)	Measured ring current (A)			
			0.4 T	0.8 T	1.2 T	1.6 T
1	2 slm H	4	17.4	15.4	16.3	16.7
1	2 slm H	6	18.1	18.6	21.6	21.6
1 and 3	2 slm H	4	33.2	33.2	28.3	21.1
1 and 3	1.5 slm H	4	33.3	32.9	25.8	17.4
1 and 3	2 slm H	6	41.7	41.4	37.3	38.4
1 and 3	1.75 slm H and 0.25 Ar	6	41.5	41.5	41.5	36.2
1 and 2 and 3	2 slm H and 0.5 Ar	4	—	49.4	49.6	39.2
1 and 2 and 3	1.75 slm H and 0.25 Ar	6	49.2	49.4	48.6	33.6

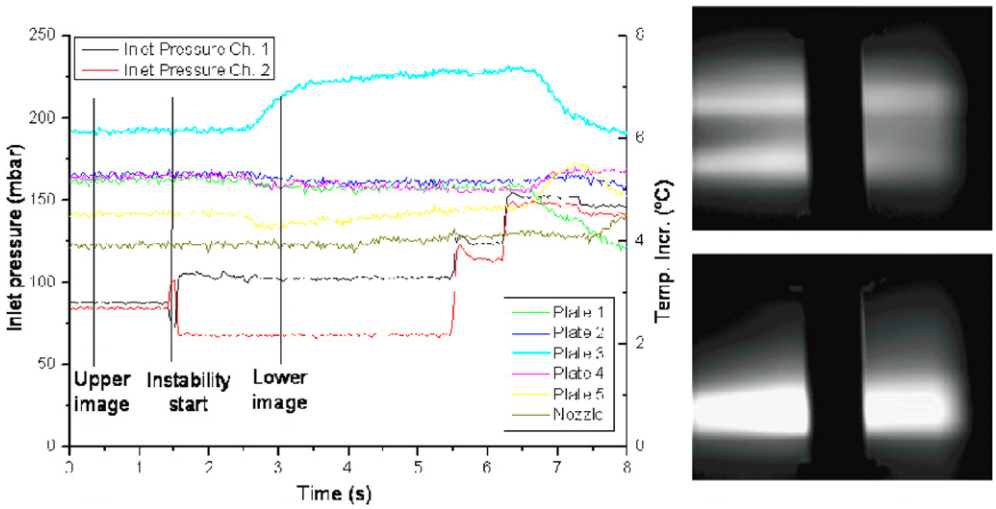

Figure 3. Time traces of the inlet pressures of channel 1 and 2 and the temperature increase of the cooling water of the different cascaded arc components revealing an instability in the operation of the two channel arc (left) and images of the plasma light (continuum radiation at 700 μs exposure time) just before (top right) and during (bottom right) such an instability.

intuitive picture once more: the plasma expands as it travels further from the source and thus a better ring filling is obtained for a larger ring distance.

3.2. Current cross talk between channels

During the experiments described above it was observed that in some cases the source output started to fluctuate. The unstable operation occurred predominantly at the highest power input levels (typically >40 kW) and with all three channels in operation. Figure 3 illustrates the nature of the fluctuations for the case of two active channels. Shown are pressure measurements and source cooling water temperature measurements as a function of time, and two visible light images of the plasma output that were recorded before and during the instability.

The two visible light images in figure 3 illustrate that the fluctuations are caused by one of the two channels occasionally turning off. This is accompanied by the other channel operating

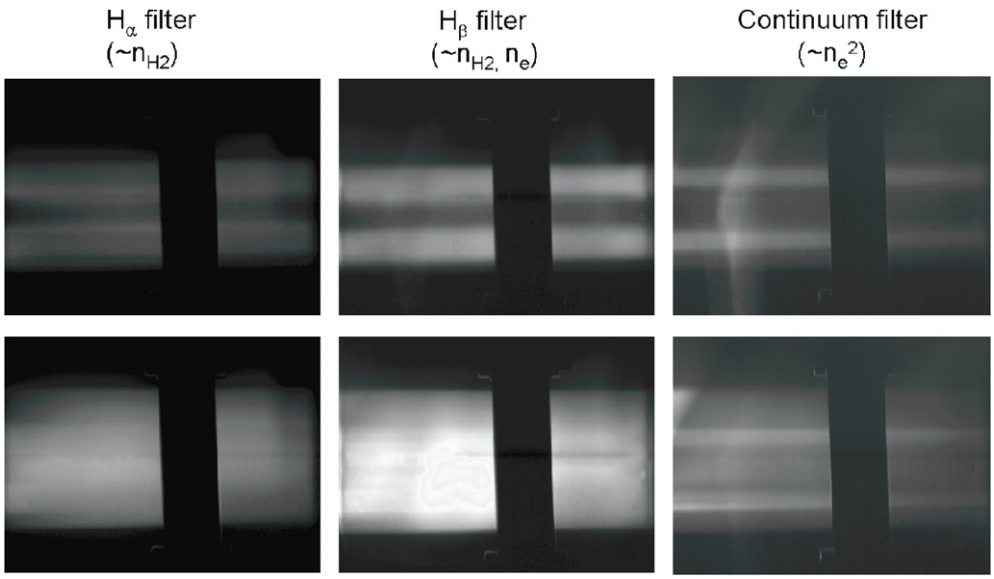

Figure 4. Fast camera images of the Balmer α, Balmer β, and continuum radiation in the red (5 μs, 200 μs and 700 μs exposure time, respectively) with three different filters before (top images) and during the biasing of the external ring (bottom images) for channels 1 and 3 operating in pure hydrogen.

more intensively. The pressure measurements indicate the same behaviour. As the pressure over channel 2 drops, apparently due to less power input along the channel, the other channel builds up more pressure, i.e. an increased power input in the channel. As the channels are physically separated, this can only mean that current attaches to the wall of channel 2 and in channel 1 a cathode spot is formed. Indeed, the temperature of the cooling water running through plate 3 increases $\sim$1 s after the internal current attachment has occurred. This time delay corresponds to the response time of the cooling water temperature measurement upon changes in the input power. Post mortem inspection of the plate revealed strong wall erosion as expected from a cathode spot.

We recall that the current crosstalk was only observed at the highest input powers. The flat I–V characteristic of the source rules out that this increases electric fields inside the channel and therewith causes arcing. We therefore conclude that the crosstalk relates to the limited cooling capacity in the present design. As can be seen in figure 1 the cooling is not symmetric for each of the channels and thus may lead to the formation of hot spots in the areas were the cooling is poorer (especially in the central region of the plates). These hot spots may initiate the emission of electrons and thus create the possibility for the current to cross through the plates from one channel to the other. This hypothesis was confirmed by adding argon to the discharge, which lowers the arc resistance and thus the discharge power. These experiments demonstrated that 40 kW was the upper limit for stable operation, irrespective of the number of driven channels.

3.3. Beam mixing and plasma rotation close to the source exit

The mixing of two individual plasma beams under the action of the external ring electrode is firstly examined qualitatively on the basis of the spontaneous plasma light emission.

Figure 4 contains images of the Balmer α, Balmer β, and continuum radiation in the red that were recorded with the ring electrode floating (upper images) and positively biased, respectively. Interpretation of these emission profiles obviously depends on the processes underlying the light excitation and is different for the three wavelength bands. H_α radiation is predominantly excited in the break up of residual gas molecules via charge exchange followed by dissociative recombination (i.e. MAR: molecular assisted recombination) as direct electron impact excitation is inefficient at plasma temperatures of about 1 eV [13]. The H_α emission is thus proportional to the product of the plasma density and molecular hydrogen density. At higher plasma densities, electron impact de-excitation of the excited levels dominates over radiative decay, which is typically true for $n_e > 5 \times 10^{19}\,m^{-3}$, as was shown by Shumack *et al* [13], and the emission becomes solely proportional to n_{H_2}. This explains the hollow emission profile per individual beam observed for the floating ring in figure 4, i.e. the strongest light emission does not occur at the centre of the jet where the electron density is highest but at the beam edges. In other words, the information obtained from H_α radiation is related to the edge of the plasma beam. The same mechanism is also producing H_β emission. However, the measured H_β emission shown in figure 4 is more peaked, which probably means that three body recombination has become significant compared with MAR at the higher densities, where it is proportional to the square root of n_e. Consequently, the emission is a complex mix relating to both n_{H_2} and n_e. The continuum radiation is proportional to the $(n_e)^2$ and indeed exhibits strong peaking in the centre of the individual channels.

Biasing of the ring induces a substantially increased emission outside of the primary beams within the volume enclosed by the ring in all three cases. This coincides with the regions in which additional power input is expected from the discharge current that is forced radially outwards in the free volume between the source and the ring. As will be confirmed below by Thomson scattering measurements, this relates to increased plasma density from extra ionization. However, the continuum image shows still signatures of the individual plasma beams although the total plasma emission indicates an efficient mixing. Moreover, the individual channels have not been displaced by $E \times B$ drift in the common radial electric field (i.e. perpendicular to the magnetic field) imposed by the ring electrode to form a helical structure as was expected at forehand from the superposition of forward plasma convection and rotation about a central axis due to $E \times B$ drift.

With the main expectation for the action of the ring, namely imposing beam mixing by twisting the individual plasma beams, not being observed in the plasma emission images, we investigated plasma beam rotation in more detail on the basis of Doppler shifts in the atomic lines [13]. Doppler shifts were determined for the H_β line to calculate plasma velocities as $v = \Delta\lambda \times c$, with v the component of the relative velocity parallel to the line of sight, $\Delta\lambda$ the line shift with respect to the original wavelength, and c the speed of light.

Figure 5 shows the results of the rotational velocity for the case of one, two and three channels (the latter with some amount of argon) obtained from the analysis of the OES measurements between the ring and the source (at 1 cm from the ring) for the case of 1.6T magnetic field and no ring biasing. We observe that the separate beams rotate around their own axes when the ring is unbiased, similar to what was observed for the one channel source in previous experiments in Pilot-PSI [13]. The spectral lines are Doppler shifted to the red at the bottom of the plasma jet and to the blue at the top, indicating rotation of the radiating species. Towards the edges of the beam the rotation is damped and the line becomes unshifted again. The direction of rotation is clockwise as viewed from the source, looking towards the target. The explanation of the beam rotation is as before. The resistivity is low in the axial direction parallel to the magnetic field and high in the radial direction perpendicular to the field so that the discharge current continues outside of the source in order to spread out in the axial

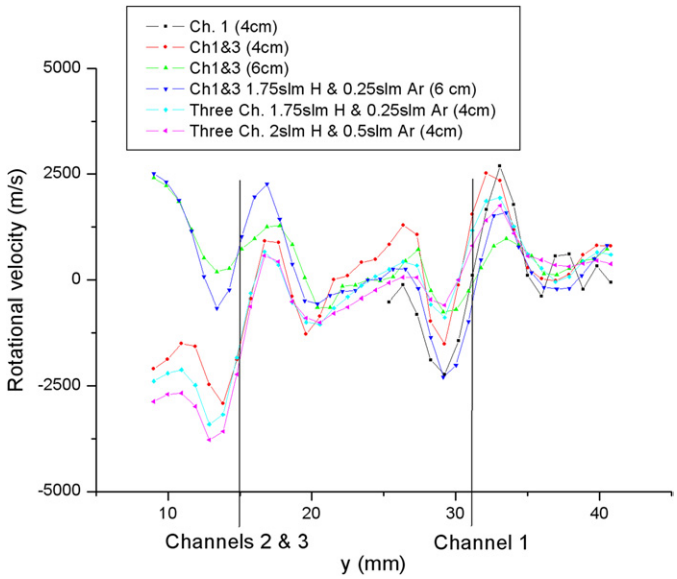

Figure 5. Rotational velocity for the case of one, two and three channels (the latter in a mixture with argon) for the case of 1.6T magnetic field and no ring biasing. Axes *y* in the direction shown in figure 1.

direction before returning to the source anode. The resistance of this current channel causes a potential build-up between the last plate of the cascaded arc and the anode. The radial electric field associated with the built-up potential can thus be estimated as the potential divided by the beam radius and was evaluated to be sufficient to produce the observed rotational velocities. The apparent difference between the data at 4 cm and at 6 cm in the third channel position is only due to different positioning of the detector for the 2 curves at 6 cm (left window of Pilot) and the 4 curves at 4 cm (right window of Pilot), due to experimental necessities.

Figure 6 shows the plasma rotation when the ring electrode is positively biased to 80V and receives part of the discharge current. It reveals an overall plasma rotation around the ring axis in addition to the signature of the individually rotating beams. Furthermore, the rotation velocity has increased significantly compared with the floating case. This is obviously due to the much higher electric fields that are induced by the positively biasing of the ring. A qualitative sketch of the rotation velocities induced by the electric field that is developed for the case of the biased ring (as viewed from the source, looking towards the target) is also shown in figure 6 for clarity. We conclude that the expected overall rotation around the axis of the ring that should favour the mixing of the three separate channels has developed.

3.4. Plasma density profiles near the target

At this point we have established the action of the ring on basis of plasma light measurements as follows:

- Extra power is put into the plasma leading to additional ionization in the volume enclosed by the ring.
- Overall plasma rotation is induced around the symmetry axis of the ring, which should favour beam mixing.
- Signatures of the individual plasma outputs remain visible in the area around the ring.

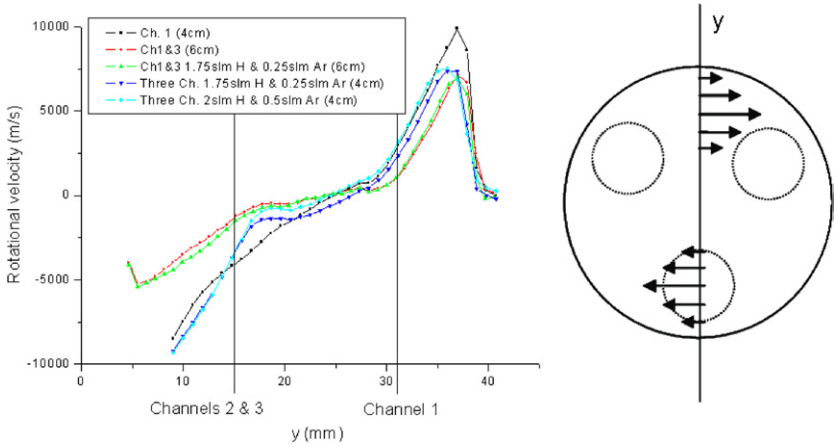

Figure 6. Rotational velocity for the case of one, two and three channels (the latter in a mixture with argon) for the case of 1.6T magnetic field and the ring biased. Sketch of the rotation velocities induced by the electric field.

Evidently, the ultimate answer on the degree of beam mixing lies in the plasma density profile as measured near the target. Figure 7 shows the density profiles for two different distances between the source and the ring and for the ring at floating and at positive bias (i.e. 'without (w/o) current' and 'with current', respectively) in the case that only one channel was in operation. Firstly, it reveals that more plasma is delivered at the target when the ring is further away from the source. This behaviour is probably fully determined by the voltage limitation in the experiment. We saw above that the ring receives more current given the voltage limitation of 90 V when it is further away from the source, which means that more power is fed to the plasma. More important is the observation that the plasma density profile changes from a one peak profile when there is no current received by the ring to a two peak profile when the ring is biased. These results confirm unambiguously that the plasma density is distributed in a ring-like manner by plasma rotation around the ring symmetry axis. We note here that the laser used for Thomson scattering passes through the centre of the vessel (figure 2) and zero position in the graph corresponds roughly with the centre of the ring electrode.

Figure 8 shows the measured density profiles for the case of two of the channels in operation (channels 1 and 3) for different conditions of the plasma and different positions of the ring. We observe that in all cases the biasing of the ring mixes the separate beams as the profile transforms from one with a single peak corresponding to the beam at the bottom centre of the ring to the broader profile that fills the entire ring. Very significant is the observation that the profiles are not hollow anymore as in figure 7. The overall rotation in combination with either less recombination or more ionization in the central region produces a homogeneous mixing near the target. This effect appears to be more significant for the case of pure Hydrogen than for the case of argon admixture where we observe a lower signal when the ring is biased. We note the truncation of the profile at $y = 8$ mm, which resulted from a drift in the alignment during the measurements and explains why the profiles do not extend to $y \approx 12$ mm as in figure 7. Taking this truncation into account, we estimate a FWHM beam width of ~2.5–3 cm on the basis of these profiles. This is more than a factor of two wider compared with the 1.2 mm nominal FWHM diameter of the one channel source [4]. The position of the ring acts as before: further away from the source means more input power given the voltage limitation and thus more ionization. The role of the gas flow is less evident. The results indicate that

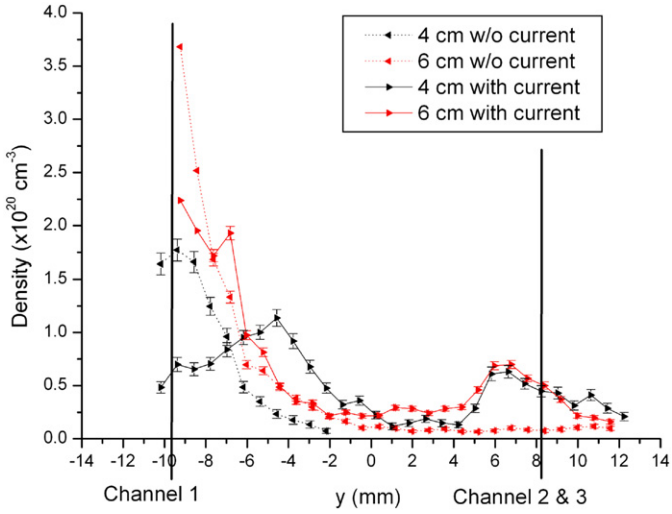

Figure 7. Density profiles measured with Thomson scattering for the case of one channel in operation. Compared are density profiles for 4 and 6 cm distance between the ring and the source as well as 'with' and 'without current' received by the ring.

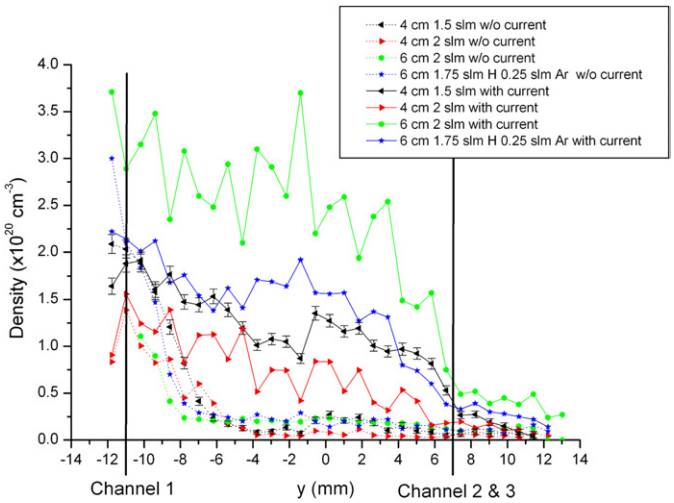

Figure 8. Density profiles for the case of channels 1 and 3 working for different plasma conditions and different positions of the ring. Measurement error under the scatter of the data. Error bars not shown for clarity.

at lower input power (i.e. with the ring closer to the source), an increased flow degrades the density at the target, perhaps due to more recombination from the higher residual gas pressure. On the other hand, increasing the gas flow in combination with more input power seems to allow for more additional ionization and is beneficial for the density at the target. This makes clear that the gas flow is to be optimized for each experimental configuration.

Finally, all three channels were operated, although with a small amount of argon added to the main hydrogen flow in order to reduce the total power load inside the source. The density profiles in figure 9 illustrate that the ring action is as before. However, the overall performance

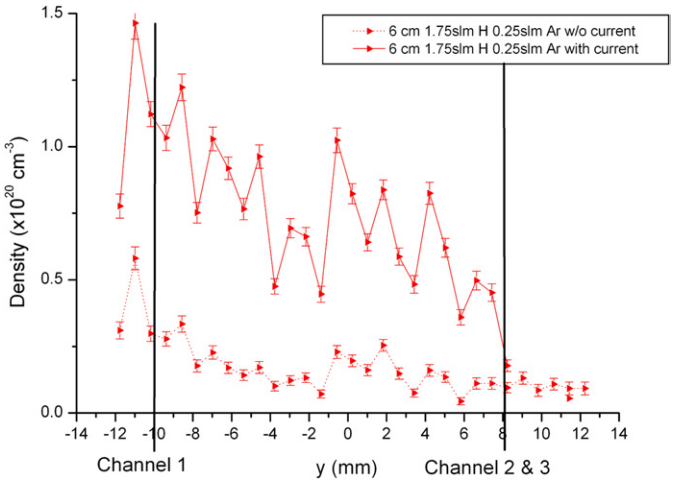

Figure 9. Density profiles for the three channels working with a small amount of argon with and without current through the ring.

has degraded by more than a factor of two. The aforementioned role of the residual gas pressure is responsible for the observed degradation. Operation of three channels at ∼2 slm per channel has increased the vessel pressure form 6 to 9 Pa, whereas optimally the vessel pressure should be at ∼1 Pa in order to limit plasma recombination [15]. This pressure increase is not expected in Magnum-PSI, the device for which the present three-channel source is being developed, as its much higher pumping speed will allow for higher gas flows without affecting the residual gas pressure significantly [16].

4. Discussion

This study encountered two factors that were limiting the operational space. Firstly, current cross talk between the channels occurred at high input powers. We conclude that the cross talk was a consequence of the simple but inefficient design of the cooling water channels in the cascaded plates. The high power loads in the central, poorly cooled, region of the plates induced high channel wall temperatures that triggered cathode spot formation. Incorporation of cooling water channels in between the discharge channels should decrease the wall temperatures and prevent current cross talk. Secondly, the plasma temperature dropped from ∼1 eV near the source to much lower values near the target, Thomson scattering data are not shown in the paper because these low temperatures are under the detection limit. This strong drop in temperature was caused by the relatively high residual gas pressure in the present experiments (∼10 Pa) due to the high gas load from operating several channels at ∼2 slm each in combination with the given available pumping capacity of Pilot-PSI. On the one hand, the drop of the temperature below 1 eV means that the hydrogen plasma becomes recombining and thus this work represents a lower limit in terms of total performance of the source and a much better performance should be expected in the Magnum-PSI device in which a much larger pumping capacity will ensure ∼1 Pa pressures even at flows of 10 slm. On the other hand, the increased pressure means more diffusion, which would mean that this work represents an overestimation in terms of overall beam width. Our experience from single channel operation at higher pressures [15] is that recombination always dominates over diffusion so that in fact the present work would still represent an underestimation in terms of overall beam width.

5. Conclusions

The rotation and mixing of the separate channels of a cascaded arc source due to the effect of a biased ring electrode placed 4–6 cm downstream of the source was studied in the Pilot-PSI. Combining the results of the plasma light measurements near the source and the density measurements near the target, we summarize for the action of positively biasing the ring electrode and therewith diverting part of the discharge current from the source anode to the ring:

- Extra power is put into the plasma leading to additional ionization in the volume enclosed by the ring;
- Overall plasma rotation is induced around the symmetry axis of the ring, which spreads the plasma density in the individual beams in a cylindrical symmetric fashion;
- The combination of the previous two effects leads to a smoothly peaked plasma profile of ∼2.5 cm FWHM, which is a factor of two wider than is nominal for a similar single channel source.

In conclusion, the externally positioned positively biased ring electrode is a suitable approach to enforce mixing via rotation of separated plasma beams.

Acknowledgment

This work was performed under collaboration between CIEMAT and FOM Euratom associations, contract number CIEMAT 09/4141.

References

[1] ITER Physics Basis 1999 *Nucl. Fusion* **39** 2137
[2] Federici G *et al* 2003 *J. Nucl. Mater.* **313–316** 11
[3] Kleyn A W, Koppers W and Lopes Cardozo N J 2006 *Vacuum* **80** 1098
[4] Van Rooij G J *et al* 2007 *Appl. Phys. Lett.* **90** 121501
[5] Van de Sanden M C M, De Regt J M, Janssen G M, Van der Mullen J A M, Schram D C and Van der Sijde B 1992 *Rev. Sci. Instrum.* **63** 3369
[6] Antar g Y, Krasheninnikov S I, Devynck P, Doerner R P, Hollmann E M, Boedo J A, Luckhardt S C and Conn R W 2001 *Phys. Rev. Lett.* **87** 065001
[7] Ohno N, Ezumi N, Takamura S, Krasheninnikov S I and Pigarov A Y 1998 *Phys. Rev. Lett.* **81** 818
[8] Meyer H, Klose S, Pasch E and Fussmann G 2000 *Phys. Rev.* E **61** 4347
[9] TechoFusion project, http://www.technofusion.org
[10] Van Rooij G J, Van der Meiden H J,'t Hoen M H J, Koppers W R, Shumack A E, Vijvers W A J, Westerhout J, Wright G M and Rapp J 2009 *Plasma Phys. Control. Fusion* **51** 124037
[11] Vijvers W A J *et al* 2009 *Fusion Eng. Des.* **84** 1933
[12] Vijver W A J, Van Gils C A J, Goedheer W J, Van der Meiden H J, Schram D C, Veremiyenko V P, Westerhout J, Lopes Cardozo N J, and van Rooij G J 2008 *Phys. Plasmas* **15** 093507
[13] Shumack A E, Veremiyenko V P, Schram D C, Van der Meiden H J, Vijvers W A J, Westerhout J, Lopes Cardozo N J and Van Rooij G J 2008 *Phys. Rev.* E **78** 046405
[14] Van der Meiden H J *et al* 2008 *Rev. Sci. Instrum.* **79** 013505
[15] Van de Peppel R J E 2007 Plasma Transport in Pilot-PSI *Bachelors Thesis* Hogeschool Rotterdam
[16] Van Eck H J N, Koppers W R, van Rooij G J, Goedheer W J, Engeln R, Schram D C, Lopes Cardozo N J and Kleyn A W 2009 *J. Appl. Phys.* **105** 063307